Theoretical investigations of electron emission after water vapour ionization by light ion impact

C. Champion and C. Dal Cappello

Laboratoire de Physique Moléculaire et des Collisions, ICPMB (FR2843),

Institut de Physique, Université Paul Verlaine-Metz, 1 Boulevard Arago,

57078 Metz Cedex 3, France

Abstract

An *ab initio* quantum-mechanical treatment is applied for treating the ionization process of water vapour by light ions. In this theoretical model, the initial state of the system is composed of a projectile and a water target described by a plane wave and an accurate one-centre molecular wave-function, respectively, whereas the final state is constituted by a slow ejected electron and a scattered projectile represented by a Coulomb wave and a plane wave, respectively. The obtained results are compared to available experimental data in terms of doubly differential cross sections (*DDCS*), singly differential cross sections (*SDCS*) and total cross sections (*TCS*). A good agreement is generally found especially for the *SDCS* and the *TCS*.

PACS codes: 34.50.Gb, 34.10.+x.

Keywords: water ionization, ion impact, theoretical cross sections, experimental comparisons

Corresponding author:

Dr. Christophe CHAMPION, Laboratoire de Physique Moléculaire et des Collisions, Université Paul-Verlaine Metz, 1 boulevard Arago, 57000 Metz, France (champion@univ-metz.fr)

phone : (00) +33-3-87-54-72-53; fax : (00) +33-3-87-54-72-57.

1. Introduction

Ionization of atoms and molecules by fast charged particles has been a matter of active research in the last two decades [1] and is nowadays a well-documented subject in many areas like atmospheric, plasma and radiation physics. However, it has been shown that experimental and theoretical data about ionization of biological systems are absolutely needed in fundamental studies like radiobiology as well as medical physics including medical imaging and radiotherapy [2]. Indeed, with the more and more regular use of ionizing radiations in medicine, it is today necessary to appraise the biological consequences of radiological examinations particularly to know, with the highest degree of accuracy, the energy deposits induced by all the radiations commonly used in radiotherapy, especially light and heavy ions.

Compared to photons, ion beams have much more favourable depth-dose distributions, the concentration of the energy deposits at the end of their range giving access to a better ballistic precision. However, the different treatments must be also compared in terms of better preservation of the healthy tissues and organ at risk in the tumour vicinity. Indeed, to improve the dose-tumour control, it is essential to conform the delivered dose to the tumour: in this way ion-beam radiotherapy, which uses the electromagnetic interaction for therapy, was suggested to treat radio-resistant tumours [3]. Thus, protons and carbon ions have been independently investigated for their depth-dose distribution particularity, namely the significant increase of the dose profile at the end of the particle range: the so-called Bragg peak. In these conditions, it appears crucial to possess accurate total and differential cross sections for describing, at best, the inelastic processes induced by heavy charged particles in the biological matter (modelled by water), in particular the ionization process whose contribution is dominant in the slowing-down of the charged particles.

In the present paper, the section 2 deals with the theoretical model developed for calculating the differential and total cross sections of water molecule ionization by stripped ions whereas the section

3 reports an extensive comparison in terms of doubly, singly and total cross sections (*DDCS*, *SDCS* and *TCS*, respectively) between the present theoretical predictions and experimental measurements. In the following sections, atomic units are used throughout unless otherwise indicated.

2. Theory

The ab-initio differential cross sections presented in this work have been calculated in the first Born approximation. The theory will be only briefly reported in the present section and for more details we refer the reader to our previous works [4-6].

2.1. The target description in the self-consistent field framework (MO-LCAO-SCF)

In the present work as well as in our previous studies devoted to water molecule ionization by electrons, protons and α-particles, the water molecule is described in its vapour phase by means of the molecular wave functions proposed by Moccia [7] whose angular part is expressed by real solid harmonics [8] whereas the radial part is developed in terms of Slater-type functions centred at a common origin, namely the oxygen atom. Under these conditions, the ten bound electrons of water molecule are distributed among five one centre molecular wave functions corresponding to the five molecular orbitals denoted 1b1, 3a1, 1b2, 2a1, and 1a1, respectively. The respective ionization potentials are 0.4954, 0.5561, 0.6814, 1.3261 and 20.5249.

2.2. The differential cross section calculation

In the ionization process of a stationary water molecule by a fast ion of charge Z_{ion} and of mass M_{ion}, the initial state of the system is characterized by a projectile of initial momentum $\vec{k}_i$, whereas the final state is characterized by a scattered ion of momentum $\vec{k}_s$ and an ejected electron of momentum $\vec{k}_e$, each of them depending on the corresponding kinetic energy through the relations

$$k_i^2 = 2*M_{ion}*E_i\,,\quad k_s^2 = 2*M_{ion}*E_s \text{ and } k_e^2 = 2E_e\,. \tag{1}$$

Thus, the non-relativistic triply differential cross section (*TDCS*) - differential in the direction of the ejected electron $d\Omega_e$, differential in the direction of the scattered ion $d\Omega_s$ and differential in the energy of ejected electron dE_e - is given by

$$\frac{d^3\sigma}{d\Omega_e d\Omega_s dE_e} = M_{ion}^2 Z_{ion}^2 \frac{k_e k_s}{k_i} |T|^2\,, \tag{2}$$

where the matrix element T describes the transition of the system {projectile + H_20} from the initial state to the final state. Then, in the so-called frozen-core approximation and by considering only one active electron (namely that which will be ejected), the matrix element T becomes

$$T = -\frac{1}{2\pi}\left\langle \psi_f(\vec{k}_s,\vec{r}_0,\vec{k}_e,\vec{r}_1)\right| \frac{1}{|\vec{r}_0-\vec{r}_1|} - \frac{1}{r_0} \left|\psi_i(\vec{k}_i,\vec{r}_0,\vec{r}_1)\right\rangle, \tag{3}$$

where the wave function $\psi_f(\vec{k}_s,\vec{r}_0,\vec{k}_e,\vec{r}_1)$ represents the system constituted by the scattered ion and the ejected electron respectively localized by the position vectors $\vec{r}_0$ and $\vec{r}_1$ with respect to the oxygen nucleus. The initial wave function $\psi_i(\vec{k}_i,\vec{r}_0,\vec{r}_1)$ is seen as the product of a plane wave function $\phi(\vec{k}_i,\vec{r}_0)$ used to describe the incident particle of position $\vec{r}_0$ with the one-centre molecular wave function $v_j(\vec{r}_1)$ (with j ranging from 1 to 5) used to describe the target active electron of position $\vec{r}_1$ expressed as a linear combination of Slater-type functions.

In the present approach based on the first Born approximation, the incident particle as well as the scattered particle is described by a plane wave function whereas the ejected electron is represented by a Coulomb wave function whose expression is given by

$$\begin{aligned} \varphi_C(\vec{k}_e, \vec{r}_1) &= \frac{\exp(i\vec{k}_e.\vec{r}_1)}{(2\pi)^{3/2}} {}_1F_1(-iZ_e/k_e, 1, -i(\vec{k}_e.\vec{r}_1 + k_e r_1)) \\ &* \exp(\frac{\pi Z_e}{2k_e}) \Gamma(1 + iZ_e/k_e). \end{aligned} \quad (4)$$

In this model, denoted in the following *FBA-CW* model, Z_e corresponds to the effective ionic charge of the remaining target seen by the escaping electron and is, in the present work, taken equal to 1 [9]. Finally, note that the molecular wave functions $v_j(\vec{r}_1)$ provided by Moccia [7] correspond to a particular orientation of the water target - expressed by means of the Euler angles (α, β, γ) (see [10-11] for more details) - what implies that the *TDCS* reported above in Eq.(2) are obviously deduced from analytical integration over the Euler solid angle of more differential cross sections (called five-fold differential cross sections) which correspond to the description of the ionization of an oriented water molecule by charged particle impact (see [10] for more details).

3. Results and discussion

The scope of the current work is to carry out a comparison between the theoretical predictions provided by our *FBA-CW* approach and some experimental available data in terms of doubly, singly differential and total cross sections for water vapour ionization by H^+, He^{2+} and C^{6+} ions. Only a few energetic conditions have been reported here and we refer the reader to our previous works for a more extensive comparison [5-6].

3.1. Doubly differential cross sections

We report in Figure 1 a comparison between the obtained theoretical results and experimental *DDCS* taken from different sources for the three particular projectile energies: a) protons of 0.3MeV [12], b) α-particles of 24MeV [13] and c) Carbon ions of 72MeV [14]. We generally observe a good agreement between the *FBA-CW* model and the measurements for all the ejected electron energies, except at small emission angles what may be explained by the fact that the process of charge transfer to the continuum (*ECC*) - called Thomas effect [15] - which causes an increase of the differential cross sections, is not included in our first Born model (see [5] for more details). However, the observed agreement is relatively good with in particular the appearance of the binary encounter peak whose position can be simply determined by kinematics considerations, namely

$$|\vec{q}\,| = \left|\vec{k}_i - \vec{k}_s\right| = k_e \Leftrightarrow \cos\theta_e = \frac{k_i^2 + k_e^2 - k_s^2}{2k_i k_e}. \qquad (5)$$

In this case, the collision is seen as a binary process in which the energy lost by the incident particle is completely transferred to the target molecular electron with the residual ion acting as a spectator [16-17]. Curiously the results reported for Carbon ions are less good, even in the binary region.

3.2. Singly differential cross sections

By integration of the *DDCS* with respect to the emission solid angle, we obtain the singly differential cross sections reported in Figure 2 and compared to available experimental data for the three incident energies reported here, namely protons of 0.3MeV, α-particles of 24MeV and Carbon ions of 72MeV. We clearly observe that the provided *SDCS* are in good agreement with the present experimental measurements in the whole ejected electron energy range except for low ejected electron energy. However, note that the agreement reported for Carbon ions is a little bit less good.

Moreover, note that the Auger electron peak is obviously not reproduced since our models include no Auger process.

3.3. Total cross sections

Figure 3 depicts a comparison between the present theoretical results and a large amount of experimental measurements for water vapour ionization by H^+, He^{2+} and C^{6+} ions. We observe that our *FBA-CW* model is able to reproduce with a reasonable agreement the existing experimental data for projectile energies greater than 100keV/amu whereas it obviously becomes invalid for lower energies where more sophisticated models are needed. However, note that the total cross section for Carbon ions, deduced from numerical integration of the *SDCS* reported in Fig. 2 c), appears to be largely lower than the theoretical calculations and it seems today of prime importance to get new experimental data in terms of differential as well as total cross sections for the $\{C^{6+} + H_2O\}$ system.

4. Conclusion

We have developed an *ab initio* model in the first Born approximation by using an accurate one-centre wave function for the water molecule. This *FBA-CW* model is able to reproduce the main part of the available experimental data for incident projectile energies greater than 100keV/amu and will be adapted for treating the ionization of larger molecules of biological interest like the nucleo-bases.

References

[1] N. Stolterfoht, R. D. Dubois and R. D. Rivarola, in: Electron Emission in Heavy Ion-Atom Collisions (Berlin: Springer), 1997.

[2] U. Amaldi and G. Kraft, Rep. Prog. Phys. **68** (2005) 1861.

[3] R. R. Wilson, Radiology **47** (1946) 487.

[4] C. Champion, Phys. Med. Biol. **48** (2003) 2147.

[5] O. Boudrioua, C. Champion, C. Dal Cappello and Y. V. Popov, Phys. Rev. A **75** (2007) 012717.

[6] C. Champion, O. Boudrioua, C. Dal Cappello, Y. Sato and D. Ohsawa, Phys. Rev. A **75** (2007) 032724.

[7] R. Moccia, J. Chem. Phys. **40** (1964) 2186.

[8] H. Trygve, P. Jorgensen and J. Olsen, in: Molecular Electronic-Structure Theory (Wiley, Chichester, West Sussex, England), 2000.

[9] C. Champion, C. Dal Cappello, S. Houamer and A. Mansouri, Phys. Rev. A **73** (2006) 012717.

[10] C. Champion, J. Hanssen and P. -A. Hervieux, Phys. Rev. A **63** (2001) 052720.

[11] C. Champion, J. Hanssen and P. -A. Hervieux, J. Chem. Phys. **121** (2004) 9423.

[12] L. H. Toburen and W. E. Wilson, J. Chem. Phys. **66** (1977) 5202.

[13] D. Ohsawa, Y. Sato, Y. Okada, V. P. Shevelko and F. Soga, Phys. Rev. A **72** (2005) 062710.

[14] D. Ohsawa and Y. Sato, private communication.

[15] L. H. Thomas, Proc. R. Soc. London, B **114** (1927) 561.

[16] M. A. Coplan, J. H. Moore and J. P. Doering, Rev. Mod. Phys. **66** (1994) 985.

[17] N. F. Mott and H. S. W. Massey, in: The Theory of Atomic Collisions (3rd ed., edited by W. Marshall and D. H. Wilkinson Oxford, Clarendon Press) 1971.

[18] M. A. Bolorizadeh and M. E. Rudd, Phys. Rev. A **33** (1986) 888.

[19] M. E. Rudd, T. V. Goffe, R. D. DuBois and L. H. Toburen, Phys. Rev. A **31** (1985) 492.

[20] M. E. Rudd, Y. K. Kim, D. H. Madison and T. J. Gay, Rev. Mod. Phys. **64** (1992) 441.

[21] M.E. Rudd, T. V. Goffe and A. Itoh, Phys. Rev. A **32** (1985) 2128.

[22] L. H. Toburen, W. E. Wilson and R. J. Popowich, Radiat. Res. **82** (1980) 27.

[23] P. S. Rudolph and C. E. Melton, J. Chem. Phys. **45** (1966) 2227.

Figure captions

Figure 1: Doubly differential cross sections for single ionization of water vapour as a function of the ejected electron emission angle. The present theoretical results are reported by solid line and compared to experimental data taken from different sources (solid symbols). Panel a): protons of 0.3MeV protons for 5 different ejected electron energies (E_e = 38.5eV, 96.2eV, 192eV, 385eV and 673eV). The experimental data are taken from [12]. Panel b): α-particles of 6.0MeV/amu for 6 different ejected electron energies (E_e = 19.2eV, 38.5eV, 96.2eV, 192eV, 385eV and 673eV). The experimental data are taken from [13]. Panel c): 72MeV C^{6+} ions for 7 different ejected electron energies (E_e = 9.6eV, 19.2eV, 38.5eV, 67.3eV, 96.2eV, 192eV and 384eV). The experiments are taken from [14].

Figure 2: Singly differential cross sections for single ionization of water vapour as a function of the ejected electron energy. The theoretical results are reported by solid (or dashed) line and compared to experimental data taken from different sources (symbols). Panel a): protons of different incident energies: 0.5MeV (open up triangles [12]), 1.5MeV (open circles [12]), 100keV (open squares [18]) and 150keV (open stars [18]). The *SDCS* for E_i = 1.5MeV and E_i = 150keV are multiplied by a factor 0.1 for clarity reasons. Panel b): α-particles of different incident energies (E_i = 24MeV, 40MeV and 60MeV, solid line [13] and E_i = 1.2MeV, 2MeV, dashed line [12]). Multiplicative factors have been used for clarity reasons. Panel c): 72MeV C^{6+} ions [14].

Figure 3: Total cross sections as a function of the incident projectile energy (in keV/amu). The theoretical results are reported by solid line and compared to experimental data taken from different sources: [18] (open diamonds), [19] (open circles) and [20] (open triangles) for protons, [21] (solid down-triangles) for ${}_3He^{2+}$, [22] (solid circles) and [23] (solid up-triangle) for ${}_4He^{2+}$, [14] (solid circle) for C^{6+} ions.

Figure 1

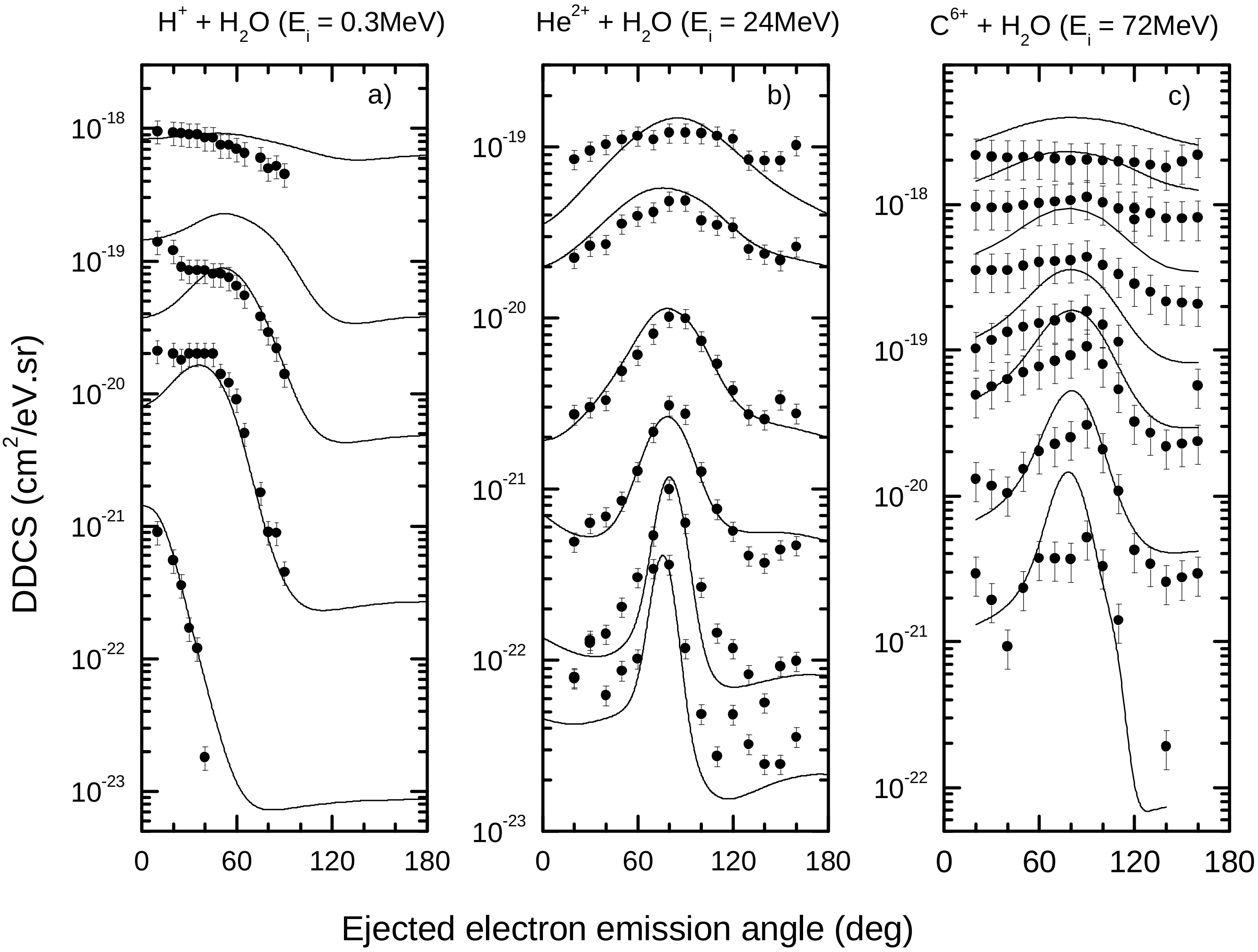
$H^+ + H_2O$ (E_i = 0.3MeV)
$He^{2+} + H_2O$ (E_i = 24MeV)
$C^{6+} + H_2O$ (E_i = 72MeV)
a)
b)
c)
DDCS (cm^2/eV.sr)
10^{-18}
10^{-19}
10^{-20}
10^{-21}
10^{-22}
10^{-23}
0
60
120
180
Ejected electron emission angle (deg)

Figure 2

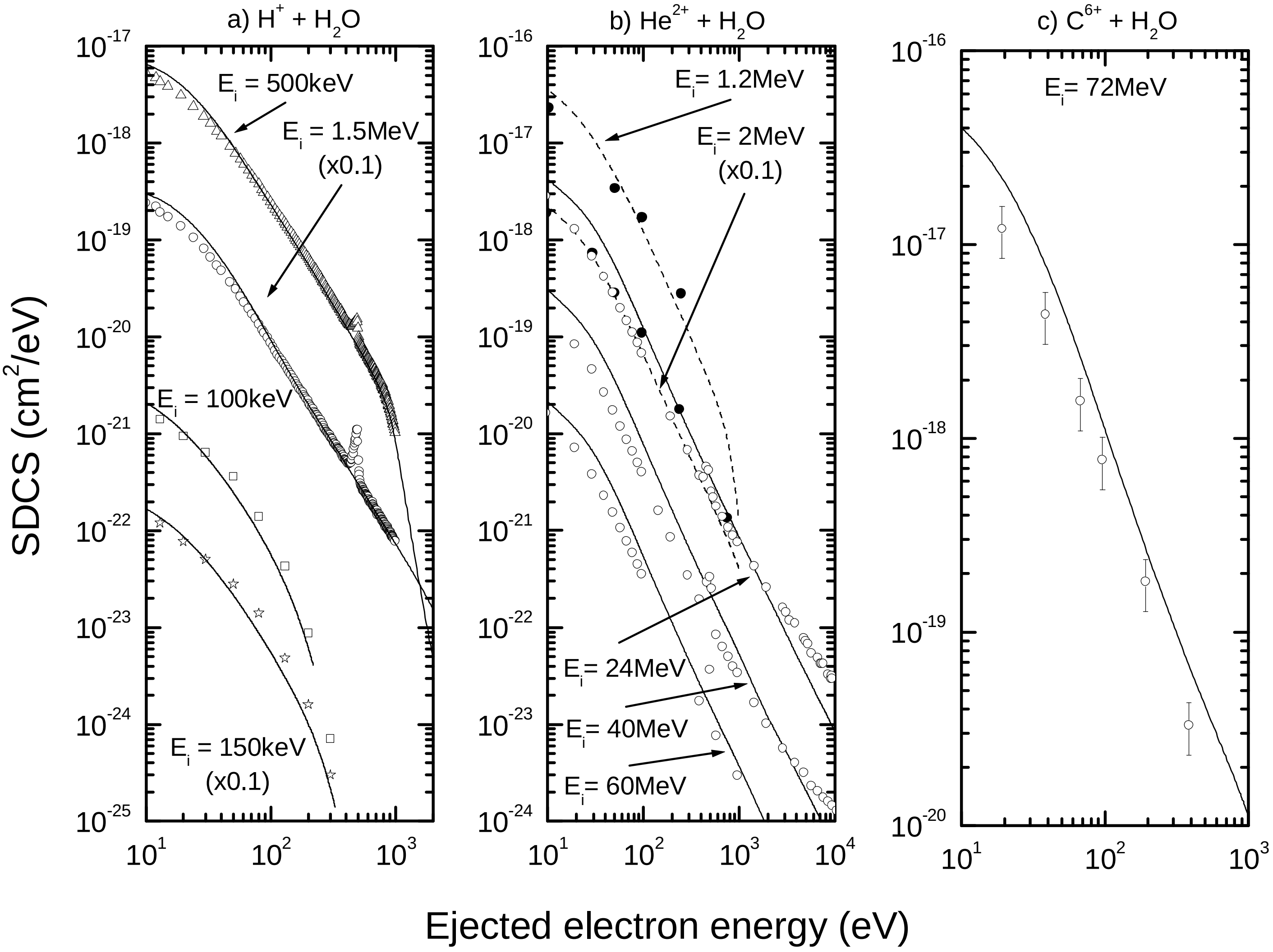
a) H$^+$ + H$_2$O
b) He^{2+} + H$_2$O
c) C^{6+} + H$_2$O
SDCS (cm^2/eV)
Ejected electron energy (eV)
E$_i$ = 500keV
E$_i$ = 1.5MeV (x0.1)
E$_i$ = 100keV
E$_i$ = 150keV (x0.1)
E$_i$= 1.2MeV
E$_i$= 2MeV (x0.1)
E$_i$= 24MeV
E$_i$= 40MeV
E$_i$= 60MeV
E$_i$= 72MeV
10^{-17}
10^{-18}
10^{-19}
10^{-20}
10^{-21}
10^{-22}
10^{-23}
10^{-24}
10^{-25}
10^{-16}
10^{1}
10^{2}
10^{3}
10^{4}

Figure 3

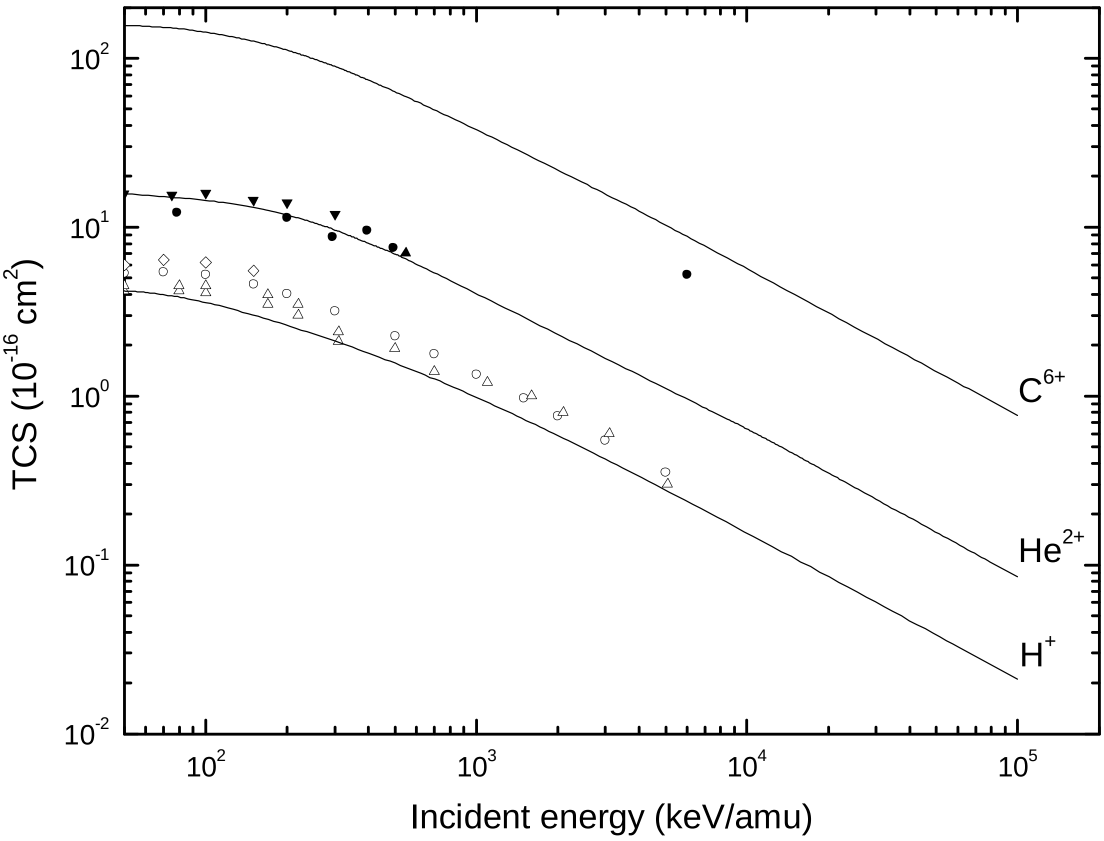
TCS (10^{-16} cm^2)
10^{2}
10^{1}
10^{0}
10^{-1}
10^{-2}
10^{2}
10^{3}
10^{4}
10^{5}
Incident energy (keV/amu)
C^{6+}
He^{2+}
H^{+}